Neural Correlates of Intensity Perception in Mid-Air Haptic Stimulation

Leen J. N. Almasu, Caroline Lehser, Daniel Schmitt, Robert Lemor, and Daniel J. Strauss.

***Abstract*—This study investigates how variations in the intensity of spatiotemporally modulated ultrasonic mid-air haptic stimulation modulate the amplitude, latency, and phase synchronization of somatosensory evoked potentials (SEPs), as well as their effect on behavioral perception. Electroencephalography recordings were obtained while stimulating the index and the middle finger of the left hand across different intensity levels, and a two-interval forced choice (2IFC) behavioral task was conducted to assess perceptual discrimination. The data revealed two dominant SEP components, a negative peak around 275 ms (N275) and a positive peak around 450 ms (P450), both showing increased absolute amplitude with higher stimulation intensity. Wavelet phase synchronization analysis further demonstrated great phase-locking stability at higher intensities. These findings indicate that mid-air haptic intensity modulated both the amplitude and temporal coherence of cortical responses. The behavioral results of the 2IFC task were consistent with the neural data. Participants reliably discriminated between intensity levels that exhibited distinct SEP amplitudes, while their performance declined for intensities that exhibited similar SEP amplitudes. Together, these results suggest that SEPs provide an objective neural correlate of subjective tactile perception. The study confirms that mid-air haptic stimulation can elicit intensity-dependent cortical responses, highlighting its potential for therapeutic, diagnostic, and interactive applications (e.g., virtual and augmented reality) despite its nontraditional stimulation mechanism. To our knowledge this is the first systematic integration linking intensity-dependent cortical responses to behavioral discrimination performance in mid-air haptic stimulation.**

***Index Terms*—Electroencephalography (EEG), haptic intensity perception, mid-air haptics, phase synchronization, Somatosensory evoked potentials (SEPs)**

I. Introduction

As digital interaction continues to evolve toward virtual, augmented, and touchless interfaces, the ability to convey tactile feedback through non-contact means has become a key focus in creating more immersive digital experiences. Ultrasound mid-air haptic systems offer a method of delivering tactile sensations without direct physical contact [1]. The principle underlying these systems was demonstrated by [2] and [3], who showed that focused acoustic radiation pressure from airborne ultrasound can produce perceivable tactile stimuli in free space. Ultrasound mid-air haptic systems allow users to experience representations of tactile events, such as a button click, without ever touching a surface. Using focused ultrasound, these systems employ ultrasonic transducers to generate precise pressure points known as focal points in the air that can interact with the skin [4], making it possible to engage with virtual or physical systems through entirely contactless feedback. In contrast to conventional haptic devices that require physical contact or wearable interfaces, this approach avoids potential issues such as interference with natural movement or inconsistencies arising from skin–device coupling [5], which can introduce variability in stimulation conditions.

Several modulation techniques have been developed to generate mid-air tactile sensations using focused ultrasound. Amplitude modulation (AM) varies the acoustic pressure at a fixed focal point to generate vibrotactile sensations [6]. Lateral modulation (LM) moves the focal point rapidly in a small path, producing more pronounced sensations [7], while spatiotemporal modulation (STM) extends this principle over a larger spatial range [6]. A core differentiator of STM and AM techniques is that for AM, increasing the number of simultaneous focal points divides the available acoustic power, weakening individual points and limiting perceptibility [8]. Spatiotemporal modulation addresses this by rapidly moving a single focal point along a trajectory to generate continuous patterns [8]. Subsequently, STM enables the generation of complex shapes more efficiently than exclusively amplitude- or laterally modulated patterns [9], making it particularly suitable for applications that require strong, clearly defined mid-air sensations and rich spatial patterns. Due to this advantage, STM is considered a preferred approach for many midair haptic applications, which motivated its selection as the stimulation method in the present study.

Mid-air haptics represents an emerging domain of research, driven by its growing applications across virtual and augmented reality [10]–[12], automotive and aviation [13], [14] and medical and assistive technology [15]–[17]. Beyond functional interfaces, it is also being considered in science communication and education as a novel channel for conveying abstract or complex concepts through touch [18]. Recent work demonstrated that EEG-based models using objective physical stimulus labels can significantly outperform evaluations that

 This work was supported in part by the Bundesministerium für Forschung, Technologie und Raumfahrt (BMFTR), Germany, under Grant BMBF-FZ 03VP10843 AG, Germany. (Corresponding author: Leen J. N. Almasu.)

L. J. N. Almasu, C. Lehser, and D. J. Strauss are with the Systems Neuroscience and Neurotechnology Unit, The Center for Digital Neurotechnologies Saar (CDNS), Faculty of Medicine, Saarland University, 66123 Saarbrücken, Germany, and also with the School of Engineering, htw saar, 66117 Saarbrücken, Germany (e-mail: leen.almasu@uni-saarland.de)

D. Schmitt is with the Fraunhofer Institute for Biomedical Engineering (IBMT), Sulzbach, Germany (email: daniel.schmitt@ibmt.fraunhofer.de).

R. Lemor is with the School of Engineering, htw saar, 66117 Saarbrücken, Germany (email: Robert.Lemor@htwsaar.de)

This work involved human subjects or animals in its research. Approval of all ethical and experimental procedures and protocols was granted by the Insti tutional Review Board at Ethikkommission der Ärztekammer des Saarlandes, Saarbrücken, Germany, under Identification No. 95/21 and performed in line with the Declaration of Helsinki.

solely depend on subjective ones when evaluating haptic experiences [19]. In addition, the importance of objective neural measures with haptic systems was further argued by [20] when they demonstrated that an EEG-based evaluation of tactile processing in children with autism spectrum disorder revealed significant differences in event-related potentials that are difficult to detect with behavioral assessments alone. These findings prove that neurophysiological markers provide more reliable, quantifiable insights into sensory processing abnormalities. With growing interest in mid-air haptics and their potential utilization across neurorehabilitation and immersive applications, understanding how this novel stimulation modulates somatosensory cortical activity via somatosensory evoked potentials (SEPs) becomes essential for establishing parametric benchmarks.

Research on mid-air ultrasound haptics has primarily examined how ultrasound-based parameters influence behavioral haptic perception, including tactile intensity and emotional response. For instance, increasing the number of focal points in a stimulus reduces perceived intensity and arousal but does not significantly affect valence [9]. Amplitude strongly affects intensity and arousal perception, while frequency effects vary by site when using mid-air haptics to stimulate the face [21]. While these psychophysical methods can quantify subjective perceived stimulus intensity, they do not reveal how variations in ultrasonic stimulation parameters are encoded at the cortical level, which motivates the use of EEG-based SEP measurements. Previous work has demonstrated that mid-air haptics using AM can elicit SEPs [22], and it has been shown that in virtual reality contexts, mismatches between visual and tactile (mid-air ultrasound via STM) can further modulate SEP responses [23]. Together, these findings indicate that mid-air haptic stimulation produces measurable cortical responses that are sensitive to sensory conditions, highlighting the potential of this technology for applications such as diagnostics and neurorehabilitation. However, the neural responses to STM stimulation, as well as how variations in its parameters further shape SEP characteristics, remain largely unexplored, motivating a systematic investigation in the present study.

In the present study, an examination of how spatiotemporally modulated mid-air ultrasound stimuli applied to the fingers influences SEP waveforms is carried out. It is hypothesized that the non-contact nature of ultrasound stimulation, along with the unique working technique of spatiotemporal modulation, which is different than conventional electrical and mechanical methods, will produce characteristic SEP responses. Furthermore, the primary aim is examining the relationship between STM stimulation intensity and SEP morphology, with the goal of identifying intensity ranges that reliably evoke measurable cortical responses. By investigating the intensity differences required to produce significant changes in ERPs, and observing pressure level at which SEPs are detectable, this study provides initial neurophysiological benchmarks for tuning mid-air haptics in diagnostic assessments of tactile processing, as well as the design of reliable non-contact haptic feedback in immersive and rehabilitative environments.

II. Materials and Methods

A. Participants

Two separate experiments were conducted in this study: experiment one, a neurophysiological evaluation (19 participants, 7 females; age range 23–29 years, mean = 26.4, standard deviation (SD) = 1.74), and experiment two, a perceptual behavioral evaluation (25 participants, 11 females; age range 22–35 years, mean = 26.44, SD = 2.88). In the first experiment, seven additional participants were excluded due to excessive pre-stimulus baseline noise, characterized by high-amplitude fluctuations comparable to the SEP peaks. In the second evaluation, two additional participants were excluded because they experienced difficulties understanding or completing the task as required. To avoid participant fatigue and ensure data quality, the EEG and behavioral experiments were carried out in separate sessions, with the behavioral measurements performed only after all EEG recordings had been completed. Due to participant availability and scheduling constraints, some individuals took part in both the EEG and behavioral measurements, while others participated in only one. All participants were healthy adults with no reported medical or neurological conditions. They were fully informed about the study and their right to withdraw at any time without explanation, and each provided written informed consent prior to participation. All procedures were carried out in accordance with the Declaration of Helsinki and were approved by the local ethics committee (application 95/21, Ärztekammer des Saarlandes; Medical Council of the Saarland).

B. Experimental setup and stimuli

Experiment one

The experimental setup incorporated a range of hardware devices for stimulus delivery and signal acquisition. Mid-air tactile stimulation was delivered using an ultrasonic board (Ultraleap Stratos Explore, Ultraleap Ltd, England). EEG signals were recorded using a biosignal amplifier (g. USBamp/USB Biosignal Amplifier, g.tec, Austria) in conjunction with passive 12 mm Ag/AgCl electrodes (BME, bioMEDproducts, USA). Trigger detection was realized using a measurement microphone (XREF 20, Sonarworks, Latvia) that recorded the ultrasonic sound waves emitted by the Ultrahaptics device during stimulation. Audio input was managed using an external sound card (Scarlett 18i20, Focusrite, UK). Digital trigger signals used to synchronize the stimulation with data acquisition were generated using a trigger box (g.TRIGbox multi-mode trigger box, g.tec, Austria). A custom-designed armrest was developed to ensure participant comfort and reduce motion artifacts. It featured a hand support that positioned the index and middle fingers above the stimulation area, while adjustable Velcro braces gently secured them to minimize movement. The design allowed participants to quickly release their fingers if needed, ensuring both comfort and safety during the experiment. A picture of the armrest is illustrated in Figure 1.

Five different intensity levels of the mid-air ultrahaptics device were tested. Through spatiotemporal modulation, the device generated the tactile illusion of a focal point traveling

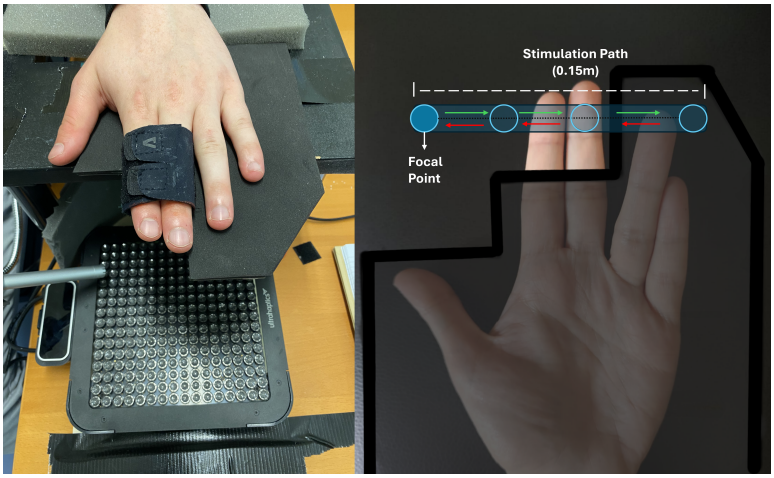

Fig. 1. Schematic of the experimental setup and spatiotemporally modulated (STM) stimulation. The illustration shows the armrest configuration, the focal point, and its trajectory along a linear path. The focal point traverses a path length of 0.15 m in a back-and-forth cyclic motion at a speed of 15 m/s within the 0.2 s stimulation period.

in a straight line. The perceived motion followed a straight line of 0.15 m, moving at a speed of 8 m/s with the focal point traversing this path repeatedly in successive cycles. A visual representation of the stimulation is shown in Figure 1. Haptic stimulation was controlled via a custom-written code, allowing the precise manipulation of stimulation parameters such as intensity, duration, and inter-stimulus timing. The stimuli were presented in a fully randomized order, with both intensity levels and inter-stimulus intervals varying unpredictably to prevent participant anticipation. Each stimulus lasted 0.2 s and was delivered at one of five intensity levels (5%, 10%, 40%, 70%, and 100%) of the device's maximum output, and inter-stimulus timing varied between 1.5 s, 2 s, and 2.5 s. In addition to the device's percentage intensity settings, physical acoustic measurements were obtained to provide an objective reference for the actual stimulation strength. The effective sound pressure levels at 5%, 10%, 40%, 70% and 100% were measured as 676, 913, 1490, 1720 and 1900 Pa, respectively, corresponding to 150.6, 153.2, 157.5, 158.7 and 159.6 dB re 20 µPa. Since acoustic intensity is proportional to the square of pressure, these values correspond to intensities of 0.10876, 0.19839, 0.52838, 0.70409 and 0.85917 W/cm², respectively.

The experiment consisted of five blocks, with each block delivering 150 stimuli over approximately six minutes, resulting in 150 trials per condition. To ensure accurate timing of the stimuli, triggers were recorded using a microphone that captured the sound emitted by the device. To avoid false triggers from sudden environmental disturbances that cross the microphone detection threshold, a digital trigger generated by the device control code was recorded simultaneously. The digital trigger served as a reference to confirm that detected events corresponded to actual stimulus delivery, allowing environmental noise to be distinguished from true stimulus triggers. The microphone was positioned within 20 cm of the focal point; given the speed of sound in air, this corresponds to a potential timing offset approximately up to 0.58 ms between stimulus emission and detection, which is negligible relative to the stimulus duration.

Experiment two

In experiment two, the setup incorporated the same mid-air tactile stimulation device and armrest structure as in experiment one. The primary focus of this work is the neuro-physiological response to STM stimulation and variations in its intensity. A behavioral study was subsequently added to verify whether the tested intensity levels were perceptually distinguishable. Establishing this perceptual context allows the observed SEPs to be interpreted in relation to the subjective tactile sensitivity. Although behavioral and subjective measures have been reported in the literature, differences in stimulation location, parameters, and modulation techniques make it difficult to directly compare results from experiment one with existent findings. To enable more valid comparisons, the behavioral measurement was therefore conducted under the same experimental conditions. A two-interval forced choice (2IFC) paradigm with four intensity levels (10%, 40%, 70%, and 100%) was implemented. Each intensity level served as a reference stimulus in a counterbalance design. All possible pairwise combinations of the four intensities were tested, and each pair was presented in both possible orders (e.g., 10% followed by 40%, and 40% followed by 10%) to control for order effects.

The task consisted of three blocks, each containing 60 randomized stimulus presentations. Within each block, every intensity pair and its inverse order were presented five times, resulting in 10 repetitions per combination per block. This design yielded 30 repetitions per stimulus pair across this measurement. Each block followed a fixed temporal structure: the first stimulus (200 ms) was followed by a 1 s inter-stimulus interval, then the second stimulus (200 ms). After the second stimulus, a response window of 5 s was given to the subjects to indicate which of the stimuli felt stronger (i.e., the target stimulus). Stimulus sequences were uniquely randomized for each block while maintaining equal distribution of intensity pairs and order combinations.

C. Data Acquisition

Experiment one

EEG data were recorded to analyze SEPs. Electrode placement followed the international 10–20 system. A total of nine electrodes were used, positioned at the following sites: C3, C4, CP3, CP4, FC3, and FC4. In addition, a ground electrode was placed on the participant's forehead, and two reference electrodes were attached to the earlobes. During the recording, participants were instructed to rest their left arm on the armrest, ensuring that their index and middle fingers were positioned directly over the center of the device, where the line tactile stimulation was delivered. To maintain attention and reduce drowsiness and daydreaming, participants were asked to silently count each stimulus they perceived and press a button after every 20 counts. The purpose of this task was solely for engagement, as the epochs that contained button presses were excluded from the final analysis to prevent them from influencing the results. Importantly, participants were not informed of the task's purpose to avoid introducing bias.

Participants were asked to keep their eyes on a cross displayed in front of them to reduce eye movement and visual distractions. Earplugs and noise-canceling over-ear headphones were also provided to block the sound produced by the mid-air ultrahaptics device and reduce external auditory distractions. All participants confirmed that they could not hear the device during the experiment. Breaks were given between blocks, during which participants were asked about internal distractions such as daydreaming, sleepiness, or any habituation to the stimuli.

Experiment two

In experiment two, no electrophysiological data were acquired. Participants were seated with their arm placed on the armrest, and as in the first experiment, it was ensured that their index and middle fingers were positioned directly above the line of stimulation produced by the device. Participants were instructed to look at a screen in front of them, which provided visual cues indicating which stimulation was currently being delivered (stimulation one/stimulation two) and when to respond. After each pair of stimulations, participants verbally indicated which stimulus they perceived as stronger by responding "stimulation one" or "stimulation two." Between the blocks participants were given a break as long as they needed.

D. Data processing and analysis

1) Data processing:

Experiment one

The EEG data were acquired at a sampling frequency of 1200 Hz. For the first five participants, recordings were initially obtained at 9600 Hz and subsequently downsampled to 1200 Hz to ensure consistency across all subjects. Impedances were below $5\,\mathrm{k}\Omega$ for all the electrodes at all times. Neurophysiological data were analyzed using MATLAB 2023b (The MathWorks, Inc.). EEG data were band-pass filtered between 1 and 30 Hz using a zero-phase FIR filter (order = 5000). For peak detection, the data were band-pass filtered between 1 and 8 Hz to facilitate the process of automatic peak detection. All channels were re-referenced to the average of the two earlobe electrodes. The data were segmented into epochs, spanning from 200 ms before each trigger to 800 ms after. Epochs associated with button presses were excluded from analysis. In addition, artifact rejection was applied using a threshold of 100 µV. Epoch-wise baseline correction was performed by subtracting the mean voltage of the 200 ms pre-stimulus period from the whole epoch. To ensure equal representation across conditions and participants, the first 100 artifact-free epochs from each condition were included in the final analysis.

2) Wavelet Phase Synchronization Stability (WPSS):

Experiment one

Phase-locked activity components in single-trial SEP responses were identified using the wavelet phase synchronization stability (WPSS). This measure is also commonly known as inter-trial phase coherence or phase-locking factor and has been successfully employed to investigate neural synchronization in the auditory [24], [25], [26], visual [27], and somatosensory domains [22].

Following the definition introduced in [24], the WPSS of a set of M single-trial signals

$$\mathcal{X} = \{x_m \in L^2(\mathbb{R}) : m = 1, \ldots, M\}$$

is given by

$$\Gamma_{a,b}(\mathcal{X}) := \frac{1}{M}\left|\sum_{m=1}^{M} e^{i\,\arg\left((\mathcal{W}_\psi x_m)(a,b)\right)}\right|, \tag{1}$$

where $(\mathcal{W}_\psi x_m)(a,b)$ denotes the continuous wavelet transform of trial x_m with respect to the complex wavelet $\psi \in L^2(\mathbb{R})$. The parameter a represents the scale (inversely related to frequency) and b is the translation (time). The absolute value $|M_{a,b}(\mathcal{X})|$ yields the synchronization index, ranging from 0 (random phases) to 1 (perfect synchronization).

In this study, we adapted the framework to our data by using the analytic Morse wavelet ($\gamma = 3$, $\beta \approx 9.87$) [28]. The sampling frequency was $f_s = 1200$ Hz, the frequency range of interest was 1–30 Hz, and 20 voices per octave were employed to ensure high frequency resolution. For statistical evaluation, the individual WPSS values computed per subject and sweep were subsequently averaged across all subjects to obtain the group-level WPSS.

To determine time-frequency points exhibiting significant phase synchronization, the Rayleigh test for circular uniformity was applied to the group-level WPSS result matrix [29]. In our framework, the inter-trial phase coherence (ITPC) served as the sample mean vector length r, calculated at each frequency f, time t, and intensity condition i.

Following Zar's formulation [29], the Rayleigh statistic was adapted as

$$R(f,t)_i = n \cdot r(f,t)_i, \tag{2}$$

where n is the number of trials contributing to the ITPC estimate. The significance of $R(f,t)_i$ was then assessed by converting it into a p-value using the approximation:

$$p(f,t)_i = \exp\left(\sqrt{1+4n+4\big(n^2-(n\cdot \mathrm{R})^2\big)} - (1+2n)\right). \tag{3}$$

This formulation was applied across the time-frequency representation of the WPSS data at the group level, with separate computations for each intensity condition i, to identify intervals of significant phase alignment, which were taken at $p < 0.05$.

3) Statistical analysis:

Experiment one

Statistical analyses were performed in R (R.4.4.1). For this experiment, the minimum and maximum peak amplitude values of all the participants were collected across all experimental conditions. Repeated measures ANOVA was used to analyze the data, with the condition as the within-subject factor. Effect sizes were reported as partial eta squared (η_p^2). The assumption of sphericity was assessed, and Greenhouse-Geisser corrections were applied. In addition, normality of residuals was checked using histograms. Post-hoc pairwise comparisons between conditions were performed using estimated marginal means with Holm adjustments for multiple testing.

Experiment two

To analyze participants' responses in the 2IFC experiment, the percentage of correct responses for each participant and each stimulus pair was computed and used as the dependent measure. Normality of residuals was checked using histograms, which indicated clear deviations from normality; therefore, a non-parametric test was used for the subsequent analysis. A Friedman test was conducted with condition as the within-subject factor to assess differences in discrimination accuracy across the different conditions. Effect size was quantified using Kendall's W. Post-hoc pairwise comparisons were further carried out using Wilcoxon signed-rank tests with Holm adjustments for multiple measurements. All previous analyses were performed in R (R.4.4.1). Subject-level performance was tested in MATLAB 2023b using the built-in function 'binocdf()', which computes the probability of observing up to a given number of correct responses under the binomial distribution, assuming random guessing (The MathWorks Inc., Natick, Massachusetts, United States). For each participant, the binomial test estimated the probability of their observed accuracy occurring by chance under the null hypothesis. This provided an additional individual-level check of significance to complement the group-level model.

III. Results

Experiment one

SEPs were recorded from multiple scalp locations following the mid-air haptic stimulation of the index and middle fingers on the left hand of the 19 participants. For later analysis, the C4 electrode was selected, as it is contralateral to the stimulated hand and positioned to detect activity from the primary somatosensory cortex [30]. SEPs were analyzed over the interval 200 ms pre-stimulus onset to 800 ms post-stimulus onset. Grand average SEP waveforms were computed for each of the five stimulus intensity levels: 5%, 10%, 40%, 70%, and 100%. To facilitate comparison of SEP amplitude across intensities, Figure 2 presents all five grand average waveforms overlaid for the three contralateral electrode sites C4, CP4, and FC4. The waveforms show two distinct peaks: a negative peak occurring approximately 275 ms (N275) after stimulus onset and a positive peak around 450 ms (P450), These latency values were averaged from the latencies of the maximum and minimum peaks across all subjects and stimulus intensities. Figure 3 presents the corresponding grand average waveforms for the three ipsilateral electrode sites C3, CP3, and FC3. Activity was also observed at similar latencies across all ipsilateral sites. Notably, increasing stimulus intensity was associated with a clear increase in the SEP absolute amplitude, indicating that the amplitude of the response is modulated by intensity. Latency also tended to decrease with higher intensity, although this effect was less consistent across conditions; detailed values are in Table I . In addition, as shown in Figure 2, the 5% intensity levels did not elicit any clear SEP peaks, suggesting that such low intensities may not reliably evoke somatosensory responses.

TABLE I
Peak Latency and Amplitude Across Stimulus Intensities

Peak	Intensity (%)	Amplitude (μV)	Latency (ms)
N	10	–1.05	341.28
N	40	–2.16	254.54
N	70	–3.92	258.71
N	100	–4.00	251.21
P	10	0.60	487.24
P	40	1.01	423.02
P	70	1.51	408.84
P	100	1.47	433.03

Moreover, grand-average WPSS was computed for each stimulus intensity across all participants, as shown in Figure 4. To assess significance, Rayleigh tests were applied at each time–frequency point, and p-values less than 0.05 were highlighted. As shown in Figure 4, higher intensities elicited larger areas of significant phase synchronization, whereas the 5% and 10% intensity levels did not show any significant effects. These results indicate that phase consistency of the somatosensory response increases with stimulus intensity, complementing the amplitude-based findings from the SEP analysis.

To get a better understanding of the relationship between the perception of different intensity levels through mid-air haptics, statistical analysis was conducted on the two dominant peak values (N275, P450) across all 19 participants.

Figure 5a and Figure 5b show the distribution of N275 and P450 amplitudes across stimulus intensities for all participants. For both peaks, absolute amplitudes generally increased with stimulus intensity. The lowest intensities (5% and 10%) elicited smaller responses, whereas the highest intensities (70% and 100%) produced larger amplitudes, with 70% showing the greatest variability across participants. The 40% intensity evoked intermediate responses. Some overlap is visible between adjacent intensity levels, particularly between 70% and 100%, consistent with the statistical analyses. Outliers are represented as points beyond the whiskers of the boxes.

For the N275, a repeated-measures ANOVA revealed a significant main effect of condition, F(4, 72) = 43.22, $p < 0.001$, Greenhouse–Geisser corrected. Post-hoc comparisons (Holm-

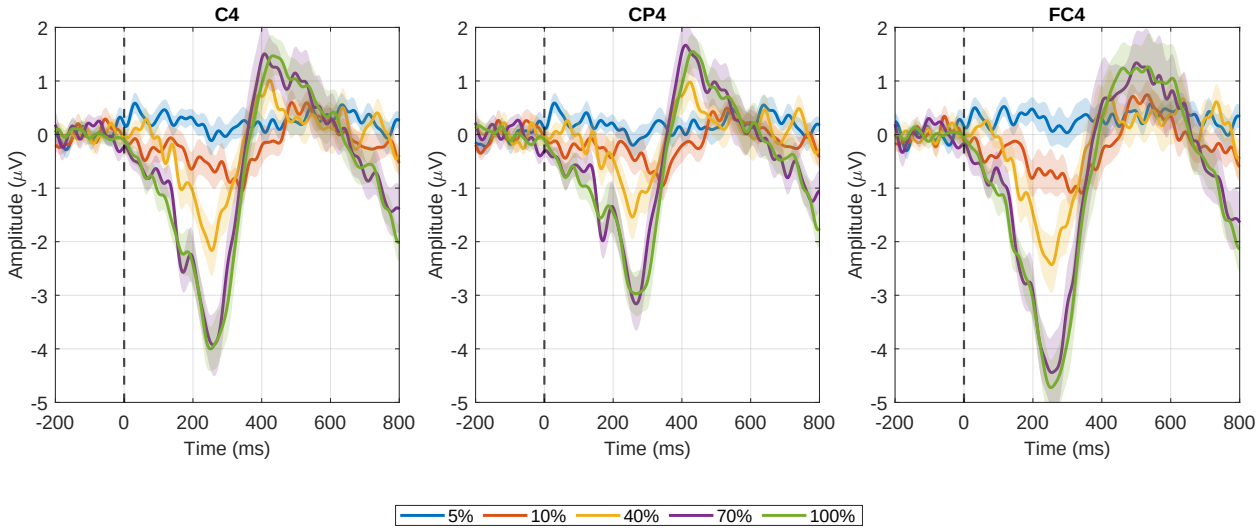

Fig. 2. This figure illustrates the grand average response across all 19 participants for each stimulus intensity level, at the contralateral electrode sites C4, CP4, and FC4. Shaded areas represent the standard error of the mean (SEM). The x-axis spans from -200 ms (pre-stimulus baseline period) to 800 ms after stimulus onset, while the y-axis represents amplitude values in μV. Two prominent peaks are evident: a negative peak occurring around 275 ms (N275) and a positive peak at approximately 450 ms (P450). The amplitude of these peaks increases with stimulus intensity. Notably, the 70% and 100% intensity levels exhibit similar amplitude values, whereas the 40% level shows a reduced amplitude. The 10% and 5% levels display minimal to no discernible peaks.

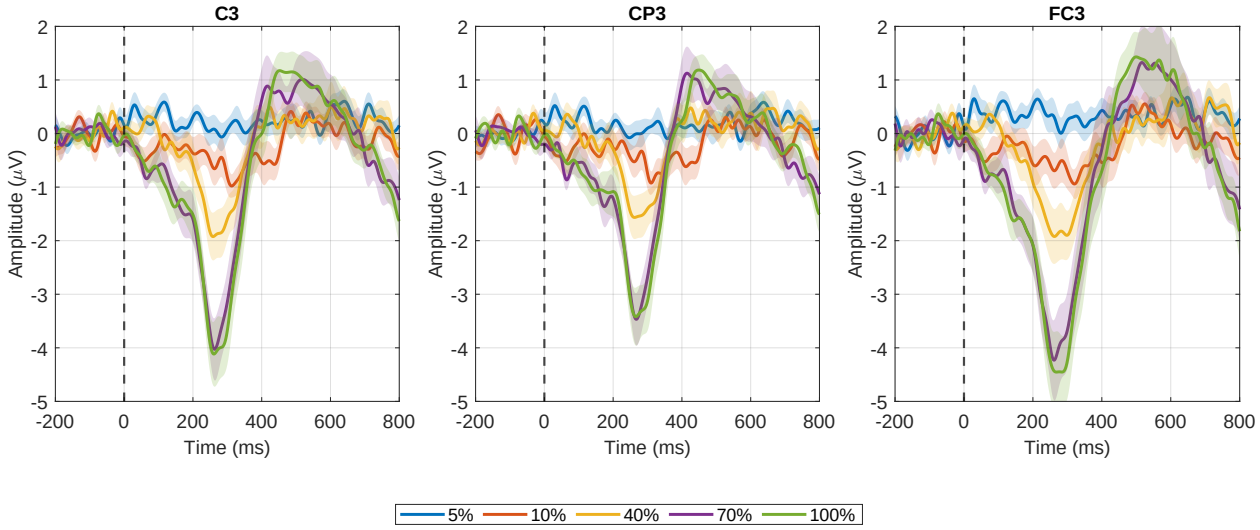

Fig. 3. This figure illustrates the grand average response across all 19 participants for each stimulus intensity level, at the ipsilateral electrode sites C3, CP3, and FC3. Shaded areas represent the standard error of the mean (SEM). The x-axis spans from -200 ms (pre-stimulus baseline period) to 800 ms after stimulus onset, while the y-axis represents amplitude values in μV. Two prominent peaks are evident across all sites. Robust activity with amplitudes approaching contralateral levels is observed at higher intensity levels (70% and 100%), while the 40% intensity level shows generally reduced amplitudes across the electrode cites. The 10% and 5% intensity levels display minimal to no discernible peaks

adjusted) showed that the amplitudes at the intensities 70% and 100% were significantly larger than at 5%, 10% and 40% (all $p < 0.01$), while no significant difference was observed between the 70% and the 100% intensities.

For the P450 peak, a significant main effect of condition was observed, F(4,72) = 13.40, $p < .001$, Greenhouse–Geisser corrected. Holm-adjusted post-hoc comparisons showed that the 70% and 100% intensities elicited significantly larger responses than both 5% and 10% (all $p < .01$). No significant differences were found between 40% and the lower intensities, nor between 70% and 100%. Detailed post-hoc comparisons for the N275 peak and the P450 peak are represented in Tables II and III.

TABLE II
POST-HOC PAIRWISE COMPARISONS FOR N275 PEAK

Contrast	Estimate	SE	df	t-ratio	Adjusted p-value
5 vs. 10	0.956	0.206	18	4.65	0.001
5 vs. 40	1.939	0.297	18	6.54	<.0001
5 vs. 70	3.572	0.423	18	8.44	<.0001
5 vs. 100	3.721	0.388	18	9.60	<.0001
10 vs. 40	0.983	0.306	18	3.21	0.010
10 vs. 70	2.616	0.450	18	5.81	0.0001
10 vs. 100	2.764	0.403	18	6.86	<.0001
40 vs. 70	1.633	0.385	18	4.25	0.002
40 vs. 100	1.782	0.342	18	5.21	0.0003
70 vs. 100	0.149	0.182	18	0.82	0.424

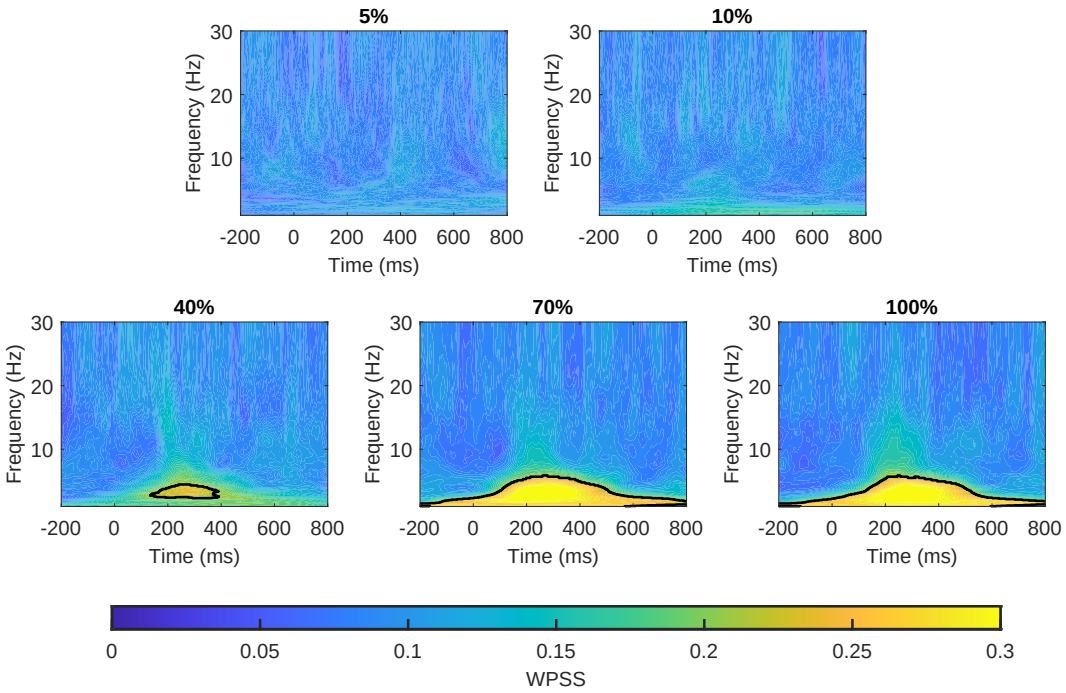

Fig. 4. Grand-average wavelet phase synchronization stability (WPSS) heatmaps for each stimulus intensity (5%, 10%, 40%, 70%, and 100%) across all participants. The x-axis represents time in milliseconds relative to stimulus onset, and the y-axis represents frequency in Hz (1–30 Hz). WPSS values are indicated by the color scale on the bottom of the heatmaps. Significant areas identified by the Rayleigh test ($p < 0.05$) are highlighted with a black contour line. Higher stimulus intensities elicit larger areas of significant phase synchronization, whereas the lowest intensities (5% and 10%) show no significant effects.

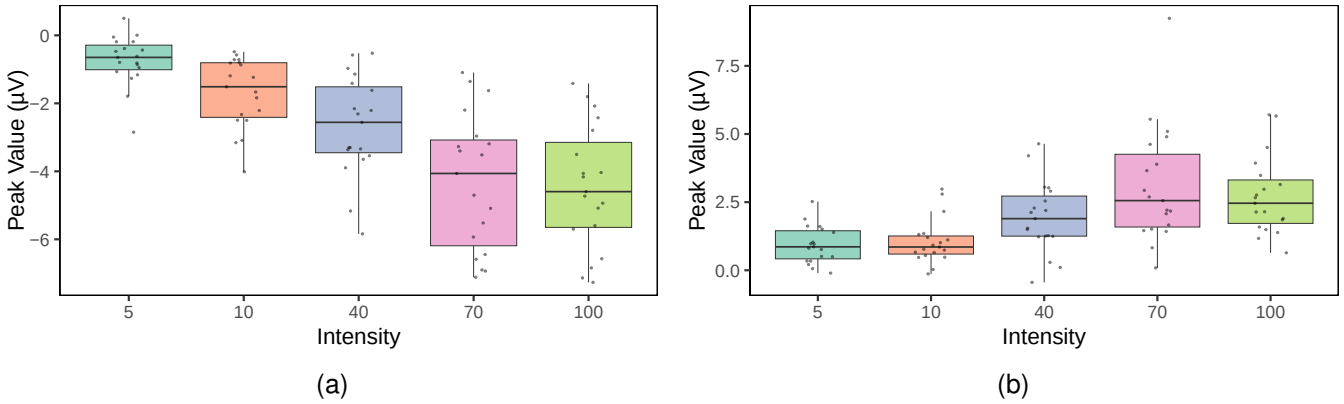

Fig. 5. Boxplots of peak values across stimulus intensities for (a) N275 and (b) P450 components. Each box shows the median, interquartile range, and overall spread of the data. Individual data points represent measurements from individual participants (N = 19), while points beyond the whiskers indicate outliers. Absolute peak values generally decreased as intensity increased. Variability was greatest at 70% intensity, with some overlap visible between adjacent intensity levels, consistent with the statistical analyses.

Experiment two

Behavioral performance in the 2IFC measurement was analyzed using the Friedman test. The analysis revealed a significant effect of stimulus pair, indicating that discrimination accuracy differed across condition pairs ($\chi^2(5) = 87.94$, $p < .001$, Kendall's W = 0.703). Following the significant overall effect indicated by the Friedman's test, post-hoc Wilcoxon signed-rank comparisons (Holm adjusted) showed that the largest performance differences occurred in the higher intensity ranges. In particular, the pairs 70-100 and 40-70 consistently showed significant differences with the other condition pairs and with each other. This indicates that distinguishing between these intensities was the most difficult for the participants. Detailed values for the post-hoc tests can be found in Table IV. These findings are consistent with the descriptive distributions shown in the boxplots in Figure 6 , where the 70-100 pair exhibits the lowest proportion of correct answers, followed by the 40-70 pair.

To assess whether the participants performed above chance, the one-tailed binomial cumulative distribution function was implemented, assuming a 50% chance level as expected in a 2IFC task. An above-chance performance was considered at a p-value < 0.05. For the stimulus pair 70%- 100%, significant differences were observed in 18 out of 25 participants,

TABLE III
POST-HOC PAIRWISE COMPARISONS FOR P450 PEAK

Contrast	Estimate	SE	df	t-ratio	Adjusted p-value
5 vs. 10	-0.112	0.195	18	-0.57	0.573
5 vs. 40	-1.003	0.339	18	-2.96	0.050
5 vs. 70	-2.145	0.488	18	-4.40	0.003
5 vs. 100	-1.779	0.367	18	-4.84	0.001
10 vs. 40	-0.892	0.333	18	-2.68	0.076
10 vs. 70	-2.034	0.480	18	-4.24	0.004
10 vs. 100	-1.668	0.329	18	-5.07	0.001
40 vs. 70	-1.142	0.466	18	-2.45	0.099
40 vs. 100	-0.776	0.321	18	-2.42	0.099
70 vs. 100	0.366	0.297	18	1.23	0.466

TABLE IV
POST-HOC PAIRWISE COMPARISONS BETWEEN THE STIMULUS PAIRS IN THE 2IFC BEHAVIORAL MEASUREMENT

Contrast	W Statistic	Adjusted p-value
10–100 vs. 10–40	38	0.685
10–100 vs. 10–70	7.5	0.596
10–100 vs. 40–100	120	0.185
10–100 vs. 40–70	210	0.000924
10–100 vs. 70–100	325	0.000189
10–40 vs. 10–70	12	0.238
10–40 vs. 40–100	122	0.327
10–40 vs. 40–70	221	0.002
10–40 vs. 70–100	325	0.000189
10–70 vs. 40–100	133	0.041
10–70 vs. 40–70	228	0.000924
10–70 vs. 70–100	325	0.000189
40–100 vs. 40–70	223	0.001
40–100 vs. 70–100	325	0.000189
40–70 vs. 70–100	325	0.000189

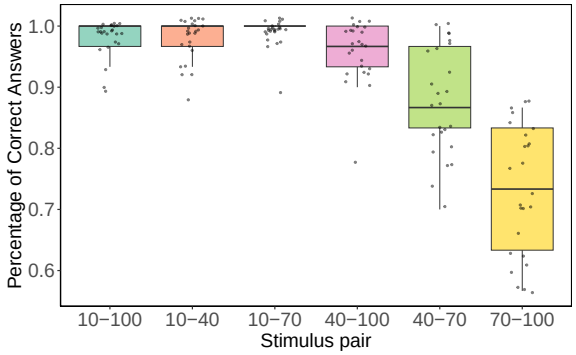

Fig. 6. Boxplots showing participants' percentage of correct responses for each stimulus pair. Each box displays the median, interquartile range, and overall spread of the data. Individual data points represent the performance of each participant. The 70–100 pair exhibits the lowest accuracy, followed by the 40–70 pair, indicating that distinguishing the intensity levels within these higher-range pairs was most difficult for participants.

suggesting that the remaining 7 participants performed below chance, likely indicating that their responses were primarily based on guessing. In contrast, for all the other stimulus pairs, significant differences were found across all participants, indicating performance above chance and suggesting that participants were not relying on guessing in these conditions.

IV. DISCUSSION

This study aimed to investigate the effects of STM mid-air haptic stimulation on SEPs elicited on the fingers and to examine how varying the perceived intensity of this stimulation modality influences SEP responses. Additionally, a 2IFC test was implemented to validate the perceptual discrimination of the intensities used and assess whether the results of the neural measurements aligned with participants' behavioral perceptions. Physical measurements, including the actual sound pressure levels produced by the device, were also recorded to determine how the physical output corresponded with both neural and behavioral responses.

The SEPs recorded in this study revealed two prominent peaks, a negative peak around 275 ms (N275) and a positive peak around 450 ms (P450). As stimulus intensity was reduced, the absolute amplitudes of these peaks generally decreased, indicating modulation of SEP amplitude by stimulus intensity of mid-air haptic ultrasound stimulation. Numerous studies have shown that varying stimulus intensity modulates SEP components at different stages of neural processing. In general, higher stimulus intensities produce larger SEP amplitudes, with the pattern of modulation depending on both the type and strength of the stimulation. For example, one study found that the early components of the SEPs (latencies $< 120ms$) remained unchanged, whereas the later components increased non-linearly with stimulus amplitude when the participants' index fingertips were stimulated using a mechanostimulator [31]. This suggests that intensity is encoded primarily in later processing steps. Another study examined SEPs in response to vibro-tactile stimulation of the right index finger and showed that both the peak values and the peak-to-peak amplitudes of the SEPs increased proportionally with the stimulus intensity [32]. Furthermore, [33], which used air-puff stimulation of the palm, found that early SEP components (e.g., P27-N35) were most strongly correlated with physical intensity, whereas later components aligned more closely with subjective ratings of perceived strength. Collectively, these results indicate that SEP features carry information about stimulus intensity, a pattern evident in the findings of this study.

The wavelet phase synchronization stability demonstrated a consistent reduction in phase locking stability within significant activity regions as intensity diminished, as determined using the Rayleigh test. These findings demonstrate that stimulus intensity modulates not only the amplitude but also the temporal phase locking of SEP components across different intensity levels of the mid-air haptics stimulation. This is in line with previous research on tactile processing, where [34] showed that higher friction during mechanical stimulation of the fingertip induced stronger and more localized phase coherence in late somatosensory potentials, underscoring that tactile stimulus properties can shape cortical synchronization across different modalities of touch.

Somatosensory evoked potentials (SEPs) elicited by finger stimulation have been characterized through literature. Typically, electrical stimulation of the median nerve induces the following components: N20, P30/P35, N60/P60, P100, P120, N140 [30] [35] [36]. Multiple studies have examined differences between electrical and vibrotactile stimulation under comparable conditions. For example, vibrotactile stimulation elicits a similar sequence of SEP components as

electrical stimulation, but with systematically delayed latencies and distinct early cortical responses, while mid- to long-latency morphology remains largely comparable [37]. The two modalities also engage different cortical pathways, with vibrotactile responses reflecting selective Pacinian activation and electrical stimulation producing broader, more generalized cortical activity [37]. In addition, the characteristics of cortical responses can vary within the same stimulation modality depending on the stimulus pattern. For example [38], showed that mechanical tactile stimulation with simple global patterns primarily activates the primary somatosensory cortex, while more complex sequential patterns recruit additional areas such as the primary motor cortex, demonstrating that stimulus patterns can modulate both evoked potentials and cortical oscillations. Interestingly, the latencies and waveform morphology observed in the results of this study are inconsistent with typical vibrotactile stimulation but rather closely approximate the N2-P2 vertex complex that is usually observed in laser-evoked potentials (LEPs) [39] [40]. LEPs are usually associated with nociceptive stimulation, but it has been shown that they are not nociceptive-specific and that they can be elicited by non-painful tactile, auditory, and visual stimuli [41]. This provides a strong framework for interpreting the N2-P2 complex elicited by the STM mid-air haptic stimulation as a salience-related cortical response. The N2-P2 vertex complex has also been observed in SEPs that were recorded in response to pulsed ultrasound, which was seen to evoke distinct waveform morphologies and modulate cortical activation depending on stimulus parameters, including the recruitment of multiple somatosensory processing regions [42]. In a recent study, [22] revealed the possibility of evoking SEPs in response to mid-air haptic stimulation on the palm using amplitude modulation, which showed that this stimulation technique can evoke SEPs distinguishable from a no-stimulation condition. In a follow-up study, [23] integrated mid-air ultrasound haptics into a multi-modal (visual-tactile) setup within a VR environment. Here, the stimulation was applied to the fingers while participants experienced visual cues, and the results showed significant differences between match and mismatch conditions. Building on this line of research, the present study applies spatiotemporal modulation stimuli to the fingers and, to our knowledge, represents the first systematic investigation of cortical responses to this more complex form of stimulation within a single sensory modality. By focusing on unimodal processing, this work aims to provide a clearer characterization of the neural correlates of such stimulation and to contribute toward a more structured framework for its evaluation. This approach may also inform future efforts to develop more objective indices of perception in contexts where subjective reporting is limited.

The effective pressure values at 5%, 10%, 40%, 70%, and 100% were measured as 676, 913, 1490, 1720 and 1900 Pa (corresponding to 150.6, 153.2, 157.5, 158.7, and 159.6 dB re 20 μPa), respectively. Because acoustic intensity is proportional to the square of the pressure, the intensity values corresponding to these pressures are 0.10876, 0.19839, 0.52838, 0.70409 and 0.85917 W/cm². The pressure difference between 70% and 100% is 180 Pa (0.9 dB), this translates to only a 22% increase in acoustic intensity, which may explain why no significant differences in SEP peak amplitudes were observed between these two levels. In contrast, the pressure difference between 40% and 70% is 230 Pa (1.2 dB), corresponding to a 33% increase in acoustic intensity, which aligns with the significant SEP amplitude differences found between these levels. Although the study was not designed to precisely determine the just noticeable difference (JND) in SPL-related SEP modulation, these results suggest that the JND may lie somewhere between 0.9 dB and 1.2 dB. Further research is needed to confirm this range. There are studies that explored JND in mid-air haptics through subjective or behavioral experiments. For instance, [43] examined JND by varying acoustic pressure intensity and rotation frequency. They reported a noticeable difference between intensity levels of 1 (2000 Pa) and 0.715 (1430 Pa), which correspond to 160 dB SPL and 157.1 dB SPL—a 2.9 dB difference. However, their study involved spatiotemporal modulation using a different shape (circle), a different location (palm), and additional factors like frequency, making it substantially different from the stimulation used in our study. Similarly, [44] investigated how well participants could detect differences in intensity and frequency of mid-air haptic patterns by measuring JNDs. They found that users required at least a 12.12% change in intensity and a 0.51 Hz change in frequency to perceive a difference reliably, based on reference values of 100% intensity and 2 Hz frequency. But again, their stimulation method and target location differ significantly from ours, making direct comparisons difficult.

The behavioral and EEG measurements were obtained from partially different participant pools, which does not permit a direct within-subject integration of behavioral and neural outcomes. Nevertheless, the behavioral study was conducted under similar stimulation and setup conditions, allowing assessment of whether the perceptual trends observed behaviorally are similarly expressed in the EEG-derived objective measures. This serves as a psychophysical validation of the stimulation levels used in the SEP recordings. Pilot testing confirmed that 10% stimulation was consistently perceptible to participants, whereas 5% intensity was not reliably detected. This justified excluding the 5% condition from the main behavioral task to avoid ambiguity while establishing 10% as the effective perceptual baseline. In this 2IFC paradigm, participants were required to indicate which of two successive stimuli felt stronger, thereby providing a bias-reduced measure of their ability to discriminate between the selected intensity levels. The behavioral data show a pattern that closely matches the SEP responses. Specifically, no significant difference in SEP peak amplitudes was observed between the 70% and 100% stimulation levels, which aligns with the behavioral results showing that participants had only limited ability to reliably discriminate between these two intensities. In contrast, a significant difference in SEP amplitudes between the 40% and 70% conditions is reflected in the behavioral data, where participants demonstrated higher discrimination accuracy. This convergence suggests that subjective perceptual judgments are closely aligned with the underlying neurophysiological responses. The lack of differentiation between the 70% and

100% stimulation levels may be explained by a perceptual saturation effect, whereby increases in physical intensity no longer produce proportional changes in perceived intensity, or alternatively, by the possibility that the difference between these levels falls below the just noticeable difference threshold. Within this framework, the 2IFC experiment serves as an important validation step, indicating that the SEP patterns correspond to behaviorally meaningful intensity differences that cannot be inferred directly from the existing literature, given the heterogeneity of stimulation modalities and experimental setups. It cannot be determined whether changes in SEPs were caused by physical intensity or perceived intensity since both increased together. However, the behavioral results still validate that our tested intensity levels produced reliable perceptual differences, confirming the relevance of the observed SEP modulations.

Overall, the results of this study demonstrate that changes in spatiotemporally modulated mid-air haptic stimulus intensity can be objectively detected using SEPs, not only through amplitude differences but also via phase-locking measures. Importantly, the SEP findings align with the participant's behavioral perception, indicating that SEPs provide a reliable neural correlate of behavioral performance. This suggests the SEPs offer a powerful and objective means of assessing subjective tactile perception, with potential applications for evaluating and optimizing mid-air haptic stimulation in VR and AR environments. Overall, these findings highlight the remarkable complexity of somatosensory evoked potentials, which are influenced by multiple interacting parameters such as stimulus modality, perceived intensity, and affective valence. The differences observed between mid-air haptics and direct contact stimulation emphasize that SEP responses cannot be directly compared across modalities, especially when factors like perceived danger or discomfort can further modulate cortical responses. Consequently, while mid-air haptic stimulation provides a promising tool for evoking measurable SEPs, its results may not be directly translatable to other forms of tactile or nociceptive input. Nonetheless, this study contributes valuable insights into the intricate dynamics of haptic perception, helping to illuminate a small part of the complex neural processes underlying somatosensory experience.

V. Conclusion

This study provides an examination of how mid-air haptic stimulation modulates somatosensory evoked potentials. The findings suggest that even contactless tactile inputs can influence neural activity in ways that reflect perceived intensity. These results highlight the inherent complexity of SEPs and the distinctive characteristics of mid-air ultrasound stimulation. Objectively characterizing these responses through SEPs is crucial for establishing the neurophysiological basis of mid-air haptics, offering insight into how the somatosensory system encodes this unique stimulation beyond behavioral perception. Further research is needed to refine these methods and clarify the parameters that shape the underlying neural dynamics. Ultimately, this work opens a path toward a deeper understanding of this stimulation modality and its integration into both scientific and applied contexts.

References

[1] I. Rakkolainen, E. Freeman, A. Sand, R. Raisamo, and S. Brewster, "A survey of mid-air ultrasound haptics and its applications," *IEEE Transactions on Haptics*, vol. 14, no. 1, pp. 2–19, 2020.

[2] T. Iwamoto, M. Tatezono, and H. Shinoda, "Non-contact method for producing tactile sensation using airborne ultrasound," in *International Conference on Human Haptic Sensing and Touch Enabled Computer Applications*. Springer, 2008, pp. 504–513.

[3] T. Hoshi, M. Takahashi, T. Iwamoto, and H. Shinoda, "Noncontact tactile display based on radiation pressure of airborne ultrasound," *IEEE transactions on haptics*, vol. 3, no. 3, pp. 155–165, 2010.

[4] Ultraleap, "Ultraleap haptics documentation," https://docs.ultraleap.com/haptics/, 2025, accessed: 2025-07-18.

[5] M. A. Akdağ, A. K. Menekşeoğlu, H. Seğmen, B. Gözek, M. D. Korkmaz, and B. Güçlü, "Measuring tactile sensitivity and mixed-reality-assisted exercise for carpal tunnel syndrome by ultrasound mid-air haptics," *Frontiers in Neuroscience*, vol. 18, p. 1319965, 2024.

[6] K. Hasegawa and H. Shinoda, "Modulation methods for ultrasound midair haptics," in *Ultrasound Mid-Air Haptics for Touchless Interfaces*. Springer, 2022, pp. 225–240.

[7] R. Takahashi, K. Hasegawa, and H. Shinoda, "Tactile stimulation by repetitive lateral movement of midair ultrasound focus," *IEEE transactions on haptics*, vol. 13, no. 2, pp. 334–342, 2019.

[8] W. Frier, D. Ablart, J. Chilles, B. Long, M. Giordano, M. Obrist, and S. Subramanian, "Using spatiotemporal modulation to draw tactile patterns in mid-air," in *International Conference on Human Haptic Sensing and Touch Enabled Computer Applications*. Springer, 2018, pp. 270–281.

[9] Z. Shen, M. K. Vasudevan, J. Kučera, M. Obrist, and D. Martinez Plasencia, "Multi-point stm: Effects of drawing speed and number of focal points on users' responses using ultrasonic mid-air haptics," in *Proceedings of the 2023 CHI conference on human factors in computing systems*, 2023, pp. 1–11.

[10] Y. Ochiai, K. Kumagai, T. Hoshi, S. Hasegawa, and Y. Hayasaki, "Cross-field aerial haptics: Rendering haptic feedback in air with light and acoustic fields," in *Proceedings of the 2016 CHI conference on human factors in computing systems*, 2016, pp. 3238–3247.

[11] L. Mulot, T. Howard, G. Gicquel, C. Pacchierotti, and M. Marchal, "Bimanual ultrasound mid-air haptics for virtual reality manipulation," *IEEE Transactions on Visualization and Computer Graphics*, pp. 1–11, 2024.

[12] A. Bhardwaj, J. Chae, R. H. Noeske, and J. R. Kim, "Tangibledata: Interactive data visualization with mid-air haptics," in *Proceedings of the 27th ACM Symposium on Virtual Reality Software and Technology*, 2021, pp. 1–11.

[13] G. Young, H. Milne, D. Griffiths, E. Padfield, R. Blenkinsopp, and O. Georgiou, "Designing mid-air haptic gesture controlled user interfaces for cars," *Proceedings of the ACM on human-computer interaction*, vol. 4, no. EICS, pp. 1–23, 2020.

[14] A. Girdler and O. Georgiou, "Mid-air haptics in aviation–creating the sensation of touch where there is nothing but thin air," *arXiv preprint arXiv:2001.01445*, 2020.

[15] G. M. Hung, N. W. John, C. Hancock, D. A. Gould, and T. Hoshi, "Ultrapulse-simulating a human arterial pulse with focussed airborne ultrasound," in *2013 35th Annual International Conference of the IEEE Engineering in Medicine and Biology Society (EMBC)*. IEEE, 2013, pp. 2511–2514.

[16] G. M. Hung, N. W. John, C. Hancock, and T. Hoshi, "Using and validating airborne ultrasound as a tactile interface within medical training simulators," in *International Symposium on Biomedical Simulation*. Springer, 2014, pp. 30–39.

[17] V. Paneva, S. Seinfeld, M. Kraiczi, and J. Müller, "Haptiread: Reading braille as mid-air haptic information," in *Proceedings of the 2020 ACM designing interactive systems conference*, 2020, pp. 13–20.

[18] D. Hajas, D. Ablart, O. Schneider, and M. Obrist, "I can feel it moving: science communicators talking about the potential of mid-air haptics," *Frontiers in Computer Science*, vol. 2, p. 534974, 2020.

[19] H. Alsuradi and M. Eid, "Eeg-based machine learning models to evaluate haptic delay: Should we label data based on self-reporting or physical stimulation?" *IEEE Transactions on Haptics*, vol. 16, no. 4, pp. 524–529, 2023.

[20] W. Wang, Y. Liu, P. Shi, J. Zhang, G. Wang, Y. Li, W. Liu, and D. Ming, "Altered tactile abnormalities in children with asd during tactile processing and recognition revealed by dynamic eeg features," *Frontiers in Psychiatry*, vol. 16, p. 1611438, 2025.

[21] R. Lan, X. Sun, Q. Wang, and B. Liu, "Ultrasonic mid-air haptics on the face: effects of lateral modulation frequency and amplitude on users' responses," in *Proceedings of the 2024 CHI Conference on Human Factors in Computing Systems*, 2024, pp. 1–12.

[22] C. Lehser, E. Wagner, and D. J. Strauss, "Somatosensory evoked responses elicited by haptic sensations in midair," *IEEE Transactions on Neural Systems and Rehabilitation Engineering*, vol. 26, no. 10, pp. 2070–2077, 2018.

[23] C. Lehser, S. A. Hillyard, and D. J. Strauss, "Feeling senseless sensations: a crossmodal eeg study of mismatched tactile and visual experiences in virtual reality," *Journal of Neural Engineering*, vol. 21, no. 5, p. 056042, 2024.

[24] D. J. Strauss, W. Delb, R. D'Amelio, Y. F. Low, and P. Falkai, "Objective quantification of the tinnitus decompensation by synchronization measures of auditory evoked single sweeps," *IEEE Transactions on Neural Systems and Rehabilitation Engineering*, vol. 16, no. 1, pp. 74–81, 2008.

[25] Y. F. Low and D. J. Strauss, "A performance study of the wavelet-phase stability (wps) in auditory selective attention," *Brain research bulletin*, vol. 86, no. 1-2, pp. 110–117, 2011.

[26] F. I. Corona-Strauss, W. Delb, B. Schick, and D. J. Strauss, "Phase stability analysis of chirp evoked auditory brainstem responses by gabor frame operators," *IEEE Transactions on Neural Systems and Rehabilitation Engineering*, vol. 17, no. 6, pp. 530–536, 2009.

[27] C. Tallon-Baudry, O. Bertrand, C. Delpuech, and J. Pernier, "Stimulus specificity of phase-locked and non-phase-locked 40 hz visual responses in human," *Journal of Neuroscience*, vol. 16, no. 13, pp. 4240–4249, 1996.

[28] J. M. Lilly and S. C. Olhede, "Generalized morse wavelets as a superfamily of analytic wavelets," *IEEE Transactions on Signal Processing*, vol. 60, no. 11, pp. 6036–6041, 2012.

[29] J. H. Zar, *Biostatistical Analysis*, 5th ed. Pearson Prentice Hall, 2010, chapter 27: Circular Distributions: Hypothesis Testing.

[30] T. Allison, G. McCarthy, C. C. Wood, and S. J. Jones, "Potentials evoked in human and monkey cerebral cortex by stimulation of the median nerve: a review of scalp and intracranial recordings," *Brain*, vol. 114, no. 6, pp. 2465–2503, 1991.

[31] D. Johnson, R. Jürgens, G. Kongehl, and H. Kornhuber, "Somatosensory evoked potentials and magnitude of perception," *Experimental Brain Research*, vol. 22, no. 3, pp. 331–334, 1975.

[32] M.-H. Choi, J.-J. Jung, J.-H. Lee, H.-S. Kim, H.-J. Kim, and S.-C. Chung, "A study on somatosensory evoked potential patterns according to various vibrotactile stimulation: frequencies and intensities," *Journal of Mechanics in Medicine and Biology*, vol. 20, no. 09, p. 2040015, 2020.

[33] I. Hashimoto, K. Yoshikawa, and M. Sasaki, "Somatosensory evoked potential correlates of psychophysical magnitude estimations for tactile air-puff stimulation in man," *Experimental Brain Research*, vol. 73, no. 3, pp. 459–469, 1988.

[34] N. Özgün, R. Bennewitz, and D. J. Strauss, "Friction in passive tactile perception induces phase coherency in late somatosensory single trial sequences," *IEEE Transactions on Neural Systems and Rehabilitation Engineering*, vol. 27, no. 2, pp. 129–138, 2019.

[35] T. Allison, G. McCarthy, and C. C. Wood, "The relationship between human long-latency somatosensory evoked potentials recorded from the cortical surface and from the scalp," *Electroencephalography and Clinical Neurophysiology/Evoked Potentials Section*, vol. 84, no. 4, pp. 301–314, 1992.

[36] N. Forss, R. Hari, R. Salmelin, A. Ahonen, M. Hämäläinen, M. Kajola, J. Knuutila, and J. Simola, "Activation of the human posterior parietal cortex by median nerve stimulation," *Experimental brain research*, vol. 99, no. 2, pp. 309–315, 1994.

[37] A. Alouit, M. Gavaret, C. Ramdani, P. G. Lindberg, and L. Dupin, "Cortical activations induced by electrical versus vibrotactile finger stimulation using eeg," *NeuroImage*, p. 121249, 2025.

[38] S. Kojima, N. Otsuru, S. Miyaguchi, H. Yokota, K. Nagasaka, K. Saito, Y. Inukai, H. Shirozu, and H. Onishi, "The intervention of mechanical tactile stimulation modulates somatosensory evoked magnetic fields and cortical oscillations," *European Journal of Neuroscience*, vol. 53, no. 10, pp. 3433–3446, 2021.

[39] H. Stowell, "Event related brain potentials and human pain: a first objective overview," *International Journal of Psychophysiology*, vol. 1, no. 2, pp. 137–151, 1984.

[40] M. Moayedi, G. Di Stefano, M. Stubbs, B. Djeugam, M. Liang, and G. Iannetti, "Nociceptive-evoked potentials are sensitive to behaviorally relevant stimulus displacements in egocentric coordinates," *ENeuro*, vol. 3, no. 3, 2016.

[41] A. Mouraux and G. D. Iannetti, "Nociceptive laser-evoked brain potentials do not reflect nociceptive-specific neural activity," *Journal of neurophysiology*, vol. 101, no. 6, pp. 3258–3269, 2009.

[42] W. Legon, A. Rowlands, A. Opitz, T. F. Sato, and W. J. Tyler, "Pulsed ultrasound differentially stimulates somatosensory circuits in humans as indicated by eeg and fmri," *PloS one*, vol. 7, no. 12, p. e51177, 2012.

[43] K. Wojna, O. Georgiou, D. Beattie, W. Frier, M. Wright, and C. Lutteroth, "An exploration of just noticeable differences in mid-air haptics," in *2023 IEEE World Haptics Conference (WHC)*. IEEE, 2023, pp. 410–416.

[44] I. Rutten, W. Frier, and D. Geerts, "Discriminating between intensities and velocities of mid-air haptic patterns," in *International Conference on Human Haptic Sensing and Touch Enabled Computer Applications*. Springer, 2020, pp. 78–86.